Article

Engineering the binding kinetics of synthetic polymer nanoparticles for siRNA delivery

Hiroyuki Koide, Tatsuya Fukuta, Anna Okishima, Saki Ariizumi, Chiaki Kiyokawa, Hiroki Tsuchida, Masahiko Nakamoto, Keiichi Yoshimatsu, Hidenori Ando, Takehisa Dewa, Tomohiro Asai, Naoto Oku, Yu Hoshino, and Kenneth J. Shea

Biomacromolecules, **Just Accepted Manuscript** • DOI: 10.1021/acs.biomac.9b00611 • Publication Date (Web): 13 Sep 2019

Engineering the binding kinetics of synthetic polymer nanoparticles for siRNA delivery

*Hiroyuki Koide,† Tatsuya Fukuta,† Anna Okishim,† Saki Ariizumi,† Chiaki Kiyokawa,† Hiroki Tsuchida,† Masahiko Nakamoto,‡ Keiichi Yoshimatsu, § Hidenori Ando,† Takehisa Dewa, || Tomohiro Asai,† Naoto Oku,† Yu Hoshino, *‡ and Kenneth J. Shea* §*

†Department of Medical Biochemistry, School of Pharmaceutical Sciences, University of Shizuoka, 52-1 Yada, Suruga-ku, Shizuoka, Shizuoka 422-8526, Japan; ‡ Department of Chemical Engineering, Kyushu University, 744 Motooka, Fukuoka 819-0395, Japan; § Department of Chemistry, University of California Irvine, Irvine, CA 92697 USA; || Department of Life Science and Applied Chemistry, Graduate School of Engineering, Nagoya Institute of Technology, Gokiso-cho, Showa-ku, Nagoya, Aichi 466-8555, Japan

KEYWORDS: polymer nanoparticle, binding kinetics, siRNA, cell penetrate peptide, lipid nanoparticle

ABSTRACT

The affinity of a synthetic polymer nanoparticle (NP) to a target biomacromolecule is determined by the association and dissociation rate constants (k_{on}, k_{off}) of the interaction. The individual rates and their sensitivity to local environmental influences are important factors for the on demand capture and release a target biomacromolecule. Positively charged NPs for siRNA delivery is a case in point. The knockdown efficacy of siRNA can be strongly influenced by the binding kinetics to the NP. Here, we show that k_{on} and k_{off} of siRNA to NPs can be individually engineered by tuning the chemical structure and composition of the NP. *N*-isopropylacrylamide-based NPs functionalized with hydrophobic and amine monomers were used. k_{off} decreased by increasing the amount of amine groups in the NP, whereas k_{on} did not change. Importantly, NPs showing a low k_{off} at pH 5.5 together with a high k_{off} at pH 7.4 showed high knockdown efficiency when NP/siRNA complexes were packaged in lipid nanoparticles. These results provide direct evidence for the premise that efficacy of a siRNA delivery vector is linked to strong affinity to the siRNA in the endosome and low affinity in the cytoplasm.

INTRODUCTION

There are now a number of examples of synthetic polymer hydrogel nanoparticles (NPs), that have been designed to capture and/or release target biomacromolecules on the basis of their intrinsic chemical composition.[1-5] The performance of abiotic NPs can be significantly influenced by not only their biomacromolecule affinity and selectivity[6-9] but also the binding kinetics (k_{on}, k_{off}) of the NP-biomacromolecule interaction.[7, 8, 10] For example, when NPs are injected into the bloodstream, they immediately become associated with serum proteins. This protein corona can significantly diminish the binding affinity of the NP to its intended target.[6-8, 10] However, if the NP-plasma protein association and dissociation rates are fast, these proteins can be exchanged, allowing NPs to interact with target proteins. It was found that both association and dissociation rates depend on the protein identity,[7] pH,[4] temperature,[5] flexibility of NPs[11] and polymer density.[12] The dissociation rate constants of NPs to the targets can also be tuned by optimizing the combination and density of charged, hydrogen-bond forming, aliphatic, and aromatic functional monomers.[4, 6, 13-15] We have been developing poly N-isopropylacrylamide (pNIPAm)-based polymer nanoparticles (NPs) that bind to target small molecules,[16] peptides[6] and proteins[17, 18] both in vitro and in vivo by incorporating combinations of hydrophobic and charged monomers in the polymer. Recently, we reported NPs that bind to the vascular endothelial growth factor ($VEGF_{165}$), an important signaling protein, by the inclusion of multiple sulfated 3,4,6S GlcNAc into the NPs.[19] The NPs inhibited tumor growth by the intravenous injection in mice.[20] It should be possible therefore, to engineer the binding kinetics of NP-biomacromolecule interactions by varying monomer composition.

Small interfering RNA (siRNA) disrupts the expression of specific genes with complementary nucleotide sequences and is being utilized in biomedical research and drug development.[21, 22] The packaging and delivery of siRNA remains challenging. There have been a number of reports of siRNA delivery vectors incorporating amine groups with significant knockdown efficacy.[23-32] It is important to form stable siRNA-vector complexes by multi-point electrostatic interactions between ammonium cations in the vector and phosphate anions in the siRNA for siRNA

delivery. After these complexes are taken up into cells via endocytosis, proton buffering capacity of the vector is also important for endsomal escape of siRNA-vector complex by the proton-sponge effect.[33-35] Under ideal conditions, siRNA should detach from the vector and make a complex with argonaute2 in the cytoplasm for the degradation of target mRNA. Therefore, the vector requires orthogonal functions; high affinity for siRNA and fast release into the cytoplasm. To address this challenge, several groups have suggested that the number and pK_a of the amine groups in the vector are critical factors for efficient gene-silencing.[26, 28, 36, 37] However, to our knowledge, there have been no reports of the relationship between binding kinetics of the siRNA vector complex (k_{on} and k_{off}) and the knockdown efficiency of target mRNA. In this report, we focused on fine-tuning the binding kinetics by varying the chemical structure and functional monomer feed ratio of the NP carrier. We show direct evidence for the relationship between binding kinetics (k_{on} and k_{off}) of the vector against siRNA and gene-silencing effect.

EXPERIMENTAL SECTION

Materials.

N-isopropylacrylamide (NIPAm), *N*,*N*,*N*',*N*'-tetramethylethylenediamine, hexadecyltrimethylammonium bromide (CTAB), 2,2'-azobis(isobutyronitrile) (AIBN) ethylenediamine (EDA), diethylenetriamine (DETA) methacryloyl chloride, di-*tert*-butyl dicarbonate, ethyl trifluoroacetate, 2M HCl/Et_2O phenylmethylsulfonyl fluoride (PMSF), 2 μg/mL leupeptin, 2 μg/mL aprotinin, and 2 μg/mL pepstatin A were purchased from Sigma Aldrich. *N*,*N*'-methylenebis(acrylamide) (BIS) and *N*-*tert*-butylacrylamide (TBAm) were from ACROS ORGANICS. Cholesterol-conjugated siRNA was purchased from Hokkaido System Science Co. (Hokkaido, Japan). The cholesterol was conjugated with siRNA at the 3'-end of the sense strand. The nucleotide sequences of siRNA with a 2-nucleotide overhang (underline) were 5′-GGCUACGUCCAGGAGCGCACC-3′ (sense) and 5′-UGCGCUCCUGGACGUAGCCUU-3′

(antisense) and 5′-GGCUACGUCCAGGAGCGCACC-3′ (sense) and 5′-UGCGCUCCUGGACGUAGCCUU-3′ (antisense, against Luc2). B16F10 murine melanoma cells were purchased from ATCC (Verginia, USA) and B16F10-Luc2 Bioware Ultra Cell Line (a luciferase-expressing cell line stably transfected with the firefly luciferase gene (Luc2, B16F10-Luc2)) were purchased from Caliper Life Sciences (Hopkinton, MA). n-octyl-β-D-glucoside was purchased from Dojindo (Kumamoto, Japan).

Synthesis of methacrylate ethylenediamine[38]

Di-*tert*-butyl dicarbonate (37.2 g, 618 mmol) in dichloromethane (DCM) (40 mL) was added dropwise to DCM containing ethylenediamine (15.0 g, 68.7 mmol) at 0 °C. Twenty-four h after stirring at r.t, DCM was evaporated and water insoluble products were removed by the filtration after the addition of water (100 mL). After the extraction with DCM (100 mL x 3), the organic layer was then dried with anhydrous Na_2SO_4 and evaporated to obtain an oily product. Then, DCM (50 mL) containing methacryloyl chloride (5.38 g, 51.43 mmol) and TEA (15.6 g, 154.3 mmol) added dropwise to the oily product (8.23 g, 51.43 mmol) and stirring for 2 h at 0 °C. After the extraction of the organic layer with water (50 mL x 3) and drying with anhydrous Na_2SO_4, evaporation of DCM was performed and the product was recrystallized with diethyl ether/hexane 3:5. In addition, recrystallization was also preformed with chloroform/diethyl ether/ hexane1:55:55. Yield: 8.0 g (47.0 mmol, 68.4 %); H1 NMR (500 MHz, $CDCl_3$): δ=1.40 (s, 9H), δ=1.98 (s, 3H), δ=3.40 (d, 4H), δ=5.40 (s, 1H), δ=5.75 (s, 1H), m/z calcd for $C_{11}H_2ON_2O_3Na$: 251.1372 (M^+Na^+); found: 251.1376

DCM (30 mL)-containing product (3.6 g, 9.8 mmol) and 2 M HCl/Et_2O (30 ml) was stirred at r.t. for 24 h. The precipitated hygroscopic salt was filtered and washed with diethyl ether. Yield: 2.0 g (9.7 mmol, 99.6 %); H^1 NMR (500 MHz, $CDCl_3$): δ=2.00 (s, 3H), δ=3.13 (t,

2H), δ=3.57 (t, 2H), δ=5.48 (s, 1H), δ=5.84 (s, 1H), m/z calcd for $C_6H_{12}N_2ONa$: 151.0847 (M^+Na^+); found .151.0852

Synthesis of methacrylate diethylenetriamine.

Diethylentriamiane (DETA, 10 g, 96.9 mmol) was protected on a primary amine by reaction with ethyl trifluoroacetate (13.7 g, 96.9 mmol, MeOH, -78 °C, for 1h). The remaining amino functional groups were next protected with di-*tert*-butyl dicarbonate (46.5 g, 213.2 mmol, 0 °C, for 2h), then, triethylamine (21.6 g, 213.2 mmol, 0 °C, for 2h) was added. The TFA protecting group was then removed by increasing the pH to 11 with conc. aq. ammonia, stirring (25 °C, overnight). The di-boc protected DETA was purified by silica gel column chromatography (DCM: MeOH: NH_3OH= 100: 50 to 100: 20: 2, v/v/v) for two times. Yield: 13.1 g (43.18 mmol, 44.6%); H1 NMR (500 MHz, CDCl3): δ=1.41 (s, 9H), δ=1.45 (s, 9H), δ=3.26 (t, 2H), δ=3.40 (t, 4H), δ=3.46 (t, 2H)

M/z calcd for $C_{14}H_{29}N_3O_4Na$: 326.2056: (M+Na+); found. 326.2049

Methacryloyl chloride (3.3 g, 32.0 mmol) and TEA (9.1 g, 90.0 mmol) were dissolved in chloroform (20 mL) and added dropwise to the di-boc-DETA (5 g, 16.5 mmol) over a period of 2 h at 0 °C. The organic layer was extracted with water (50 mL x 3) and dried over anhydrous Na_2SO_4. Chloroform was evaporated and the product was purified by silica gel column chromatography (DCM: MeOH = 100: 5 to 10: 1, v/v). Yield: 3.6 g (9.8 mmol, 59.4 %); H1 NMR (500 MHz, CDCl3): δ=1.42 (s, 9H), δ=1.45 (s, 9H), δ=1.94 (s, 3H), δ=3.31 (t, 4H), δ=3.47 (t, 4H), δ=5.36 (s, 1H) , δ=5.75 (s, 1H) m/z calcd for $C_{18}H_{33}N_3O_5Na$: 394.2318: (M+Na+); found .394.2314

A solution-containing product (3.6 g, 9.8 mmol) in DCM 30 mL and 2 M HCl/Et_2O (30 ml) was stirred at room temperature for 24 h. Then, the precipitated hygroscopic salt was filtered and washed with diethyl ether. Yield: 2.0 g (9.7 mmol, 99.6 %); H^1 NMR (500 MHz, $CDCl_3$):

δ=2.02 (s, 3H), δ=3.39 (sextet, 6H), δ=3.66 (t, 2H), δ=5.50 (s, 1H) , δ=5.89 (s, 1H) m/z calcd for $C_8H_{18}N_3O$: 172.1450: ($M+H^+$); found .172.1457

Preparation of NPs.

NPs were prepared by a modified precipitation polymerization[39] of *N*-isopropylacrylamide (NIPAm), *N,N'*-methylenebisacrylamide (Bis), *N-tert*-butylacrylamide (TBAm) and *N*-(3-aminopropyl)methacrylamide hydrochloride, methacrylated ethylendiamine (EDA) or methacrylated diethylentriamine (DETA). NIPAm, amine monomer (APM, EDA or DETA), TBAm, BIS, and CTAB (10 mg) were dissolved in ultrapure water (total monomer concentration; 65 mM). TBAm was dissolved in a small amount of ethanol before the addition. The monomers and surfactant-containing solutions were filtered and degassed by the nitrogen purge for 30 min. Then, azobisisobutyronitrile (AIBN, 6 mg/10 mL) was added to the solution under a nitrogen atmosphere for the starting the polymerization (65°C for 3 h). The synthesized NPs were purified by dialysis (changed twice a day) for 4 days.

Characterization of NPs

The hydrodynamic diameter of NP was determined in aqueous solution by dynamic light scattering (DLS) (Zetasizer Nano ZS). The temperature of the NP samples was controlled via Peltier device at 25 ± 0.1 °C. Yield and concentration of NPs were determined by measuring weight of NP after lyophilization.

Titration assay

5 ml of each NP solution (1 mg/ml in water) was bubbled by nitrogen for 30 min. Then, 10 μl of 0.01 N HCl was added into the NP solution. pH change was monitored after each injection.

Electrophoresis assay

siRNA and amine NP complex was incubated for 30 min at r.t. Then, free siRNA dissociated from NPs was separated by electrophoresis in 15% acrylamide gel. The gel was stained for 30 min in Gel Red, and siRNA was detected by a LAS-3000 mini system (Fuji Film, Tokyo, Japan).

Cell culture

B16F10 and B16F10-Luc2 cells were cultured in DME/Ham F-12 medium (WAKO, Osaka, Japan) containing 10% fetal bovine serum (FBS, Sigma-Aldrich), 100 units/mL penicillin (MP Biomedicals, Irvine, CA), and 100 μg/mL streptomycin (MP Biomedicals) in a CO_2 incubator.

siRNA uptake

siRNA uptake studies were performed as previously described.[40] Briefly, B16F10 cells (1.0×10^4 cells/well) were incubated with naked FITC-siRNA (100 nM) or FITC-labeled siRNA-C formulated in NPs or NP/siRNA-C-LNP-CPP for 24 h. After washing the cells with PBS, the cells were lysed (1 w/v% n-octyl-β-D-glucoside containing 1 mM PMSF, 2 μg/mL leupeptin, 2 μg/mL aprotinin, and 2 μg/mL pepstatin A). The FITC fluorescence intensity and protein amount were measured by a Tecan Infinite M200 microplate reader (Salzburg, Austria) (ex. 485 nm, em.

535 nm) and BCA Protein Assay Reagent Kit (PIERCE Bio- technology, Rockford, IL), respectively.

Knockdown effect

Knockdown studies were performed as previously described.[40] Briefly, B16F10-luc2 cells (5×10^3 cells/well) were incubated with sample (50 pmol of siRNA-C (siLuc2)) in the medium without antibiotics. After washing the cells, the cells were cultured in the fresh medium (with antibiotics) for 24 h. Then, luminescence and cell viability were measured with ONE-Glo Reagent (Promega, Madison, WI) and Cell Titer-Fluor Cell Viability Assay kit (Promega), respectively.

Preparation of CPP-modified NPs and siRNA complex-encapsulated lipid nanoparticles (NP/siRNA-C-LNPs-CPP)

1,2-Dipalmitoyl-sn-glycero-3-phosphoglycerol, sodium salt (DPPG) dioleoylphosphatidylethanolamine (DOPE) and cholesterol (DPPG: DOPE: Cho = 1:1:1 as a molar ratio) were dissolved in *tert*-butyl alcohol and freeze-dried. LNPs were prepared by the hydration with DEPC-treated RNase-free water and sized by extrusion 10 times through a polycarbonate membrane filter (100-nm pores, Nucleopore, Maidstone, UK). NP (75 μg) and siRNA-C (250 pmol) were incubated at 37 °C for 30 min (total 250 μL). NPs and siRNA complex-encapsulated lipid nanoparticles (NP/siRNA-C-LNPs) was prepared by freeze-thawing method.[40] The NP/siRNA-C complex (250 μL) was added to LNPs (1 mM, 750 μL) and freeze-thawed for 3 times. CPP-DOPE was modified onto the NP/siRNA-C-LNP surface (6 mol% against total lipid as molar ratio) by incubation at 37 °C for 30 min.

Confocal microscopy

B16F10 cells were seeded onto eight-well chamber slides (Nunc, Rochester, NY, USA) at a density of 1.0×10^4 cells/well and transfected with TAMRA-labeled siRNA-C (TAMRA-siRNA-C), which was complexed with NPs or NP/siRNA-C-LNP-CPP (TAMRA-siRNAC concentration was 30 pmol/0.3 ml/well). Twenty-four h after transfection with each sample, the cells were washed three times with PBS (pH 7.4) containing heparin (5 units/ml). Then, the cells were incubated in fresh medium containing Lysotracker in accordance with the manufacturer's instructions and fixed with 4% paraformaldehyde. Nuclei were stained with 4′,6-diamino-2-phenylindole (DAPI; 10 μg/ml; Invitrogen) in PBS containing 3% BSA and 0.1% saponin (Sigma-Aldrich). The localization of FITC-labeled siRNA-C in B16F10 was observed by LSM510 META confocal laser-scanning microscope (Carl Zeiss, Jena, Germany).

Quartz crystal microbalance (QCM) analysis

Interactions between the NPs and siRNA was quantified by an Affinix Q^8 QCM instrument (Initium Co. Ltd., Tokyo, Japan).[12, 18] Gold surfaces in QCM cell were incubated with piranha solution for 5 min, twice fir the surface cleaning. 3,3'-Dithiodipropionic acid (1 mM, 0.1 mL) was added to the gold surface and incubated for overnight. Then, the gold surfaces were washed with ultrapure water and added 1-ethyl-3-(3-dimethylaminopropyl)-carbodiimide (100 mg/ml) and *N*-hydroxysuccinimide (100 mg/mL) (1:1, 0.1 mL) to form *N*-hydroxysuccinimidyl esters. Amine NPs were loaded on the cells to give NPs-immobilized cells. Then, the QCM cells were washed with PBS for 3 times. siRNA-C was added onto NPs immobilized QCM cells at the concentration of 30, 100 or 300 nM. Interactions between NPs and siRNA-C were measured at (37±0.1)°C in PBS (pH 7.4). The apparent dissociation constant of NPs to siRNA-C was calculated under the assumption that all particles have the same affinity to siRNA-C.

RESULTS AND DISCUSSION

Preparation of synthetic polymer NPs for siRNA affinity

To engineer the binding kinetics of NPs to siRNA, we evaluated the contribution of both the number and spacing of amine residues on NP–siRNA binding and both dissociation rate and dissociation equilibrium constants. It was reported that spacing of positively charged amino groups in the side chain plays a key role for gene-silencing.[38] Amine monomers of methacrylated ethylenediamine (EDA) and diethylenetriamine (DETA) were used to introduce positively charged functionality (**Figure 1**). Since the synthetic NP is a poly-*N*-acrylamide derivative, DETA functionalized NPs have a different number of amine residues per side chain and the length of amine side chain differs from EDA functionalized NPs. To establish the influence of carbon number, (3-aminopropyl)methacrylamide hydrochloride (APM) was also used as an amine source. The amine groups in the NPs contribute to the electrostatic attraction to siRNA at a pH lower than the pK_a of their conjugate ammonium ions. It is also known that incorporation of hydrophobic groups in the NP is effective for creating high affinity for hydrophobic targets[6,7] and for tuning the pK_a of ammonium ions in the NPs.[41] Thus, siRNA was conjugated with cholesterol (siRNA-C) at the 3' position of the sense strand [42,43] and 40 mol% of *N-tert*-butyl acrylamide (TBAm, hydrophobic monomer) was incorporated into all NPs to create the hydrophobic interactions. Cholesterol conjugation to siRNA at the 3' position improves stability of siRNA against nuclease in the bloodstream without reduction of the knockdown effect.[42] The NPs were synthesized by free-radical copolymerization of the functional monomers with a cross-linking monomer (*N*,*N'*-methylene-bis(acrylamide) (BIS), 2 mol %) in aqueous solution containing small amounts of CTAB. AIBN was used as initiator (**Figure 1**). Summaries of NP compositions, particle sizes and ζ-potentials are given in **Table 1**. To measure protonation capacity and apparent pK_a of the NPs, an acid-base titration assay was performed (**Figure S1a-c**).[26] Both mono-amine (APM and EDA) NPs showed a single and clear neutralization point. Interestingly, APM and EDA NPs with 5 mol% of the amine monomers (NP1 and 5) showed lower average pK_a's (~7.5) than those with more than 15 mol% (~8-10). This may be due to a

less polar microenvironment around isolated amine groups in NP1 and 5 than those of NPs containing a larger number of amines.[41-44] Di-amine (DETA) NPs showed a characteristic gradual decrease in pH upon addition of 0.01N HCl due to the two different pK_a's of the DETA monomer. Due to the electrostatic repulsion of neighboring ammonium ions, apparent pK_a's of DETA NPs (<7.5) are lower than that of APM and EDA NPs. Importantly, proton capacity of NPs with the same percentage of amines was not significantly different. In addition the degree of protonation was not significantly different for each NP, ~1 at pH5.5 and ~ 0.4-0.5 at pH7.4. It was reported that both ionization behavior and proton buffering capacity are important for the proton sponge effect. [26,45-47] These results suggest that the proton sponge effect of each NP should be similar. "

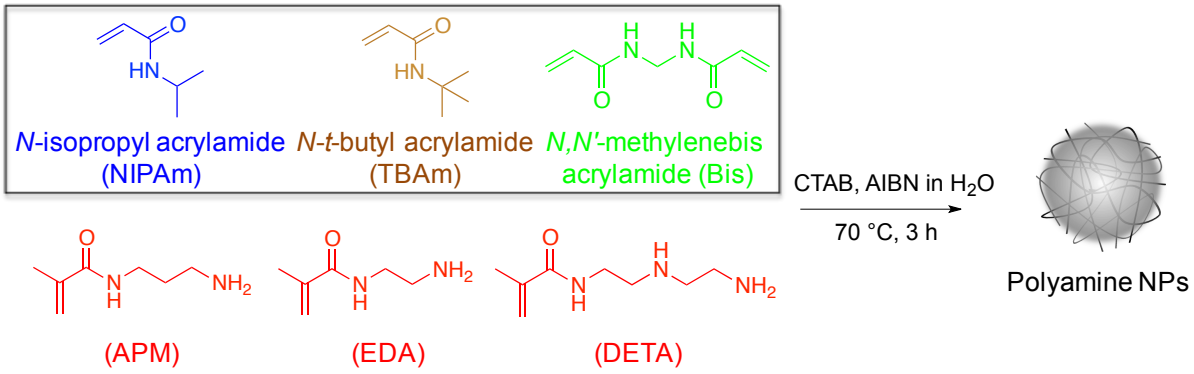

Figure 1. Preparation of amine functionalized NPs. NPs were synthesized by free radical copolymerization of functional (NIPAm, TBAm and Bis) and amine monomers in the presence of cetyltrimethylammonium bromide (CTAB, 0.694 mM) in water. Following the addition of 2,2'-azobis(isobutyronitrile) (AIBN, 2.63 mM), the polymerization was carried out at 70 °C for 3 h. NPs were purified by dialysis using 100K MW cutoff dialysis tubing. NP numbering is correlated with the functional amine monomer.

Table 1. Monomer compositions, sizes, ζ-potentials and electrophoretic mobilities of NPs.

	NIPAm	APM	TBAm	Bis	Size (nm)	PDI	ζ-potential (mV)	Mobility (μmcm/Vs)
NP1 (5% APM)	53	5	40	2	56 ± 8	0.19 ± 0.12	47 ± 4	3.7 ± 0.3
NP2 (10% APM)	48	10	40	2	62 ± 8	0.16 ± 0.10	39 ± 4	3.1 ± 0.3
NP3 (15% APM)	43	15	40	2	61 ± 7	0.22 ± 0.05	42 ± 2	3.3 ± 0.2
NP4 (20% APM)	38	20	40	2	74 ± 19	0.27 ± 0.06	24 ± 2	1.9 ± 0.2

	NIPAm	EDA	TBAm	Bis	Size (nm)	PDI	ζ-potential (mV)	Mobility (μmcm/Vs
NP5 (5% EDA)	53	5	40	2	58 ± 5	0.25 ± 0.04	36 ± 8	2.8 ± 0.6
NP6 (10% EDA)	48	10	40	2	44 ± 6	0.22 ± 0.03	34 ± 5	2.7 ± 0.4
NP7 (15% EDA)	43	15	40	2	57 ± 7	0.24 ± 0.07	35 ± 10	2.7 ± 0.8
NP8 (20% EDA)	38	20	40	2	78 ± 10	0.29 ± 0.13	37 ± 4	2.9 ± 0.3

	NIPAm	DETA	TBAm	Bis	Size (nm)	PDI	ζ-potential (mV)	Mobility (μmcm/Vs)
NP9 (5% DETA)	53	5	40	2	53 ± 4	0.27 ± 0.04	44 ± 3	3.4 ± 0.2
NP10 (10% DETA)	48	10	40	2	52 ± 6	0.20 ± 0.04	37 ± 9	2.9 ± 0.7
NP11 (15% DETA)	43	15	40	2	52 ±16	0.24 ± 0.10	40 ± 4	3.1 ± 0.3
NP12 (20% DETA)	38	20	40	2	53 ± 4	0.27 ± 0.10	36 ± 3	2.8 ± 0.2

Evaluation of NP affinity to siRNA-C

We next evaluated the siRNA interaction with NPs by electrophoretic analysis. (**Figure 2a**). After incubating NPs (5 μg) and siRNA-C (0.35 μg) in water (pH 5.5), the unbound siRNA-C was separated on a 15% polyacrylamide gel. siRNA incubated with NPs which have only 5 mol% of APM, EDA, and DETA (NP1 (5% APM), NP5 (5% EDA) and NP9 (5% DETA), respectively) showed a strong band at the same migration distance as the one without NPs (lane C), indicating the NPs had little affinity for siRNA-C. However, NPs with more than 10 mol% of amine monomers (NP2-4, NP6-8 and NP10-12, respectively) captured the siRNA-C almost quantitatively, indicating the importance of the density of charged groups. It was reported that capture of siRNA by a NP requires inclusion of a critical amount of cationic groups,[45] indicating charge density is important for siRNA binding. We suggest that the positively charged monomers are uniformly dispersed in the NPs due to electrostatic repulsion. Therefore, the charge density of 5 mol% cationic monomer containing NPs is insufficient for siRNA binding. To confirm the contribution of the hydrophobic interaction to NP-siRNA binding, an electrophoretic assay was performed with siRNA that was not conjugated with cholesterol or NPs containing a low percentage of hydrophobic monomer (TBAm). The association of cholesterol free siRNA with DETA NPs was lower than siRNA-C (**Figure S2a**). However, APM and EDA NPs still had a strong interaction indicating electrostatic interactions dominate siRNA interactions with these NPs. In the case of low TBAm containing NPs, we focused on the DETA NPs. When the TBAm percentage decreased from 20% to 0% (**Table S1**), free siRNA bands gradually appeared (**Figure S2b**). Since hydrophobic interactions between cholesterol and TBAm should assist the interaction between siRNA and DETA containing NPs, the combination of electrostatic and hydrophobic interactions are important to achieve high affinity between these NPs and siRNA-C (**Figure S2c,d,e**) and highlights the difference between di-amine and mono-amine containing NPs.

To account for the difference in binding affinity, we measured association and dissociation rate constants of NPs against siRNA-C at pH 5.5 (endosomal pH) and pH 7.4 (cytoplasm pH). siRNA-C was injected into amine NPs immobilized on quartz crystal microbalance (QCM) cells at several concentrations (**Figure 2b**). Both the binding rate (relaxation time of the binding process) and the binding amount of siRNA-C depended on the concentration of siRNA-C. The time courses of the frequency changes of the QCM in the siRNA-C binding events were fitted to a single exponential function (**Figure S3**).[48] ΔF, ΔF_∞; Frequency change at time t or ∞ after injection, τ; relaxation time.

In the Langmuir adsorption model, the binding process is defined as eq. (1), and the increasing amount of siRNA/binding-site complex per unit time is given by eq. (2). In this study, the amount of siRNA in solution is in large excess relative to the number of binding sites on the surface of the QCM (eq. (3)), so the number of siRNA/binding-site complexes at time t after injection is given by eq. (4). Then, eq. (2) is rewritten as eq. (5); here, we defined τ as eq. (6). Thus, the amount of siRNA/binding-site complex formed at time t after injection is given by eq. (7). In the QCM measurement, the frequency change at time ∞ (ΔFmax) corresponds to eq. (8) and the frequency change at time t after injection (ΔF) corresponds to the number of siRNA/binding-site complexes. Thus, eq. (7) is used synonymously with eq. (9). Therefore, the relaxation time (τ) of siRNA binding can be obtained from curve fitting by a single exponential function using eq. (9) at different siRNA concentrations (30–300 nM). Association and dissociation rate constants (k_{on} and k_{off}, respectively) are given as the slope and y-intercept of the linear correlations between siRNA concentrations and the reciprocal of the binding relaxation time according to eq. (6). The dissociation constants (K_d) are given as k_{off}/k_{on}.

Frequency changes in the siRNA binding processes were fit well by the single exponential function (**Figure S3**). The reciprocals of the binding relaxation times (τ), which were obtained from the exponential function, were proportional to the concentrations of siRNA (**Figure 2**).

From those results, we analyzed the binding kinetics by approximating them by the Langmuir adsorption model.

(1) $siRNA + Binding\ site \underset{k_{off}}{\overset{k_{on}}{\rightleftarrows}} siRNA \cdot Binding\ site$

(2) $d[siRNA \cdot Binding\ site]/dt = k_{on}[siRNA][Binding\ site]-k_{off}[siRNA \cdot Binding\ site]$

(3) $[siRNA]_0 >> [Binding\ site]_0$

(4) $[Binding\ site]=[Binding\ site]_0 - [siRNA \cdot Binding\ site]$

(5) $d[siRNA \cdot Binding\ site]/dt = -1/\tau\ ([siRNA \cdot Binding\ site]-k_{on}[siRNA]_0[Binding\ site]_0/-k_{on}[siRNA]_0 + k_{off})$

(6) $1/\tau = k_{on}[siRNA]_0 + k_{off}$

(7) $[siRNA \cdot Binding\ site] = (1-exp(-t/\tau))k_{on}[siRNA]_0[Binding\ site]_0/(k_{on}[siRNA]_0+k_{off})$

(8) $\Delta F_{max} = k_{on}[siRNA]_0[Binding\ site]_0/(k_{on}[siRNA]_0+k_{off})$

(9) $\Delta F = \Delta F_{max}(1-exp(-t/\tau))$

Plotting the reciprocal of the binding relaxation time (t) against siRNA-C concentration gives a linear correlation between siRNA-C concentration and τ^{-1} for each NP (**Figure 2b**). The binding process can be approximated as Langmuir-type binding isotherm shown in (10). Apparent association/dissociation rate constants (k_{on} and k_{off}) of NPs are given as the slope and y-intercept of the linear correlations (11).[11,12]

siRNA + NP □ siRNA・NP (10)

$\tau^{-1} = k_{on}$ [siRNA] $+k_{off}$ (11)

Apparent association and dissociation rate constants (k_{on} and k_{off}) and dissociation equilibrium constants K_d ($=k_{off}/k_{on}$) at pH 5.5 and pH 7.4 are shown in **Table 2**. The kinetic analysis revealed that k_{on} of all NPs shows approximately $10\times10^3 M^{-1}s^{-1}$ at pH 5.5 and $20\times10^3\ M^{-1}s^{-1}$ at pH 7.4 although the amine percentage and number of amine groups in each NP were different. k_{off}

could be reduced by increasing the percent of amine monomers, this results in a stronger affinity (smaller K_d value) to the siRNA. Both k_{on} and k_{off} of siRNA to APM and EDA NPs (NP2 (10% APM), 4 (20% APM), 6 (10% EDA), 8 (20% EDA)) can be equally accelerated (2~3 times) by increasing pH. However, k_{off} of siRNA to DETA NPs (NP10 (10% DETA), 12 (20% DETA)) increased 6-8 times by the pH change despite a 1.5-fold increase in k_{on}. Eventually, K_d of DETA NPs was dramatically increased compared with that of APM and EDA NPs. It is possible therefore to engineer NPs, which have the same binding affinity but a different exchange rate by changing the pH. We find it is possible to use pH to accelerate only the dissociation rate constant (k_{off}) by optimizing amine structure and percentage. The result is to increase binding affinity by about one order of magnitude.

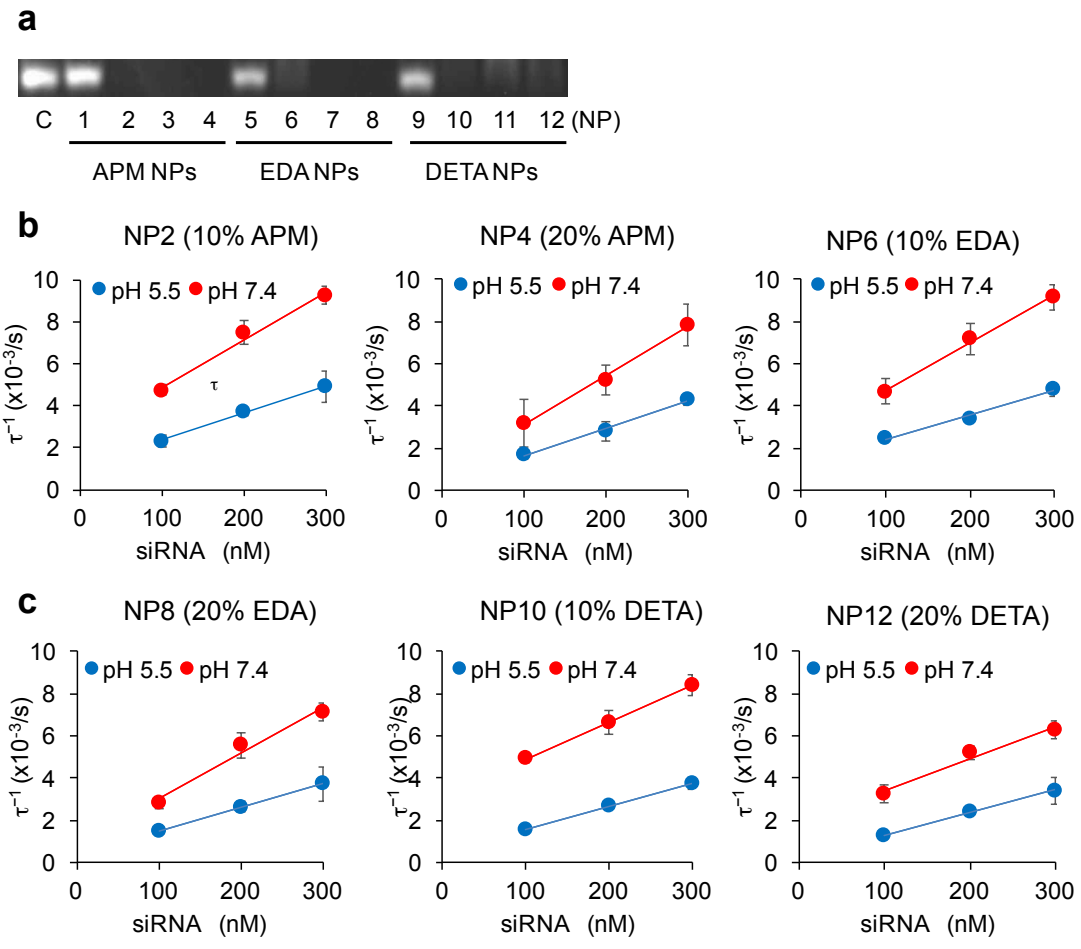

Figure 2. Binding affinity of amine NPs to siRNA-C. (a) Electrophoretic analysis of NP-siRNA-C interaction. siRNA-C which is not attached to 5 μg of NPs was separated by electrophoresis in 15% polyacrylamide gel. C; Naked siRNA-C. Remaining lanes siRNA-C + indicated NPs. (b,c) Plots of binding relaxation time (τ) of NP2 (10% APM), 4 (20% APM), 6 (10% EDA) 8 (20% EDA), 10 (10% DETA) and 12 (20 % DETA) at pH 7.4 (open circle) or 5.5 (black circle).

Table 2. Association and dissociation rate constants and equilibrium constants of NPs.

	pH 5.5			pH 7.4		
	k_{on} ($10^3 M^{-1} \cdot s^{-1}$)	k_{off} (10^{-3} s^{-1})	K_d (nM)	k_{on} ($10^3 M^{-1} \cdot s^{-1}$)	k_{off} (10^{-3} s^{-1})	K_d (nM)
NP2 (10% APM)	13	1.06	82	23	2.63	114
NP4 (20% APM)	13	0.30	23	23	0.78	34
NP6 (10% EDA)	12	1.26	105	22	2.53	115
NP8 (20% EDA)	11	0.38	35	21	0.89	42
NP10 (10% DETA)	11	0.50	45	17	3.16	186
NP12 (20% DETA)	11	0.23	21	15	1.92	128

Preparation of NPs and siRNA-C complex-encapsulated lipid nanoparticles

To evaluate the importance of the binding kinetics of NPs against siRNA for efficient knockdown, it is important to design experimental conditions in which the amount of siRNA-C uptake into the cells is equal in each NP/siRNA-C complex. To equalize the siRNA uptake, NP/siRNA-C complexes were encapsulated in lipid nanoparticles (LNPs, 1,2-Dipalmitoyl-sn-glycero-3-phosphorylglycerol sodium salt (DPPG) : Cholesterol : 1,2-Dioleoyl-sn-glycero-3-phosphoethanolamine (DOPE)=1:1:1) by freeze-thawing NP/siRNA-C and LNP complexes three times (NP/siRNA-C-LNP, **Figure 3a**).[40,49,50] Incorporation of DOPE, fusogenic lipids, into the LNP has been shown to promote endosomal release by increasing the interaction between the LNP and endosomal membranes.[51-54] To deliver the NP/siRNA-C-LNP into the cell, the NP/siRNA-C-LNP was modified with DOPE-conjugated cell penetrate peptide (CPP, DOPE-conjugated RRRRRRGGRRRRG, NP/siRNA-C-LNP-CPP). It was reported that the peptide delivers LNPs to the cell via heparan sulfate-mediated endocytosis and macropinocytosis.[55] Initially NPs were approximately 80 nm but after freeze-thawing the NP/siRNA-C complex, they were no longer visible (**Table 3, Figure S4**). The results indicate that most of the NPs were encapsulated into the LNPs.

Table 3. Size, PDI and ζ-potential and electrophoretic mobilities of NP/siRNA-C-LNP-CPP.

	Size (d.nm)	PDI	ζ-potential (mV)	Mobility (μmcm/Vs)
NP2 (10% APM)/siRNA-C-LNPs-CPP	342 ± 25	0.21 ± 0.05	33 ± 6	2.6 ± 0.5
NP4 (20% APM)/siRNA-C-LNPs-CPP	335 ± 23	0.20 ± 0.02	34 ± 7	2.7 ± 0.5
NP6 (10% EDA)/siRNA-C-LNPs-CPP	364 ± 14	0.21 ± 0.07	30 ± 2	2.3 ± 0.2
NP8 (20% EDA)/siRNA-C-LNPs-CPP	305 ± 21	0.21 ± 0.04	36 ± 3	2.8 ± 0.2
NP10 (10% DETA)/siRNA-C-LNPs-CPP	366 ± 15	0.22 ± 0.03	33 ± 5	2.6 ± 0.4
NP12 (20% DETA)/siRNA-C-LNPs-CPP	357 ± 19	0.31 ± 0.03	38 ± 1	3.0 ± 0.1

Importance of binding kinetics for siRNA release into cytoplasm and significant knockdown

To demonstrate cellular uptake of siRNA-C wrapped by LNP-CPP, FITC-conjugated siRNA-C was used. FITC-siRNA-C mixed with only DOPE-conjugated CPP was used as a control. Twenty-four hours after the addition of NP/siRNA-C-LNP-CPP onto B16F10 cells (siRNA concentration: 50 nM), fluoresce intensity of siRNA was measured. siRNA uptake into the cells was not significantly different in each NP (**Figure S5**). Importantly, the NP/siRNA and NP/siRNA-C-LNP-CPP complexes have little toxicity at 10 μg/ml NP concentration. (**Figure S6a,b**). We next demonstrated the knockdown effect of NP/siRNA-C-LNP-CPP. siRNA-C against luciferase (Luc2, siLuc2-C) and luciferase overexpressing B16F10 (B16F10-Luc2) were used for the assay. NP/siLuc2-C-LNP-CPP was incubated with B16F10-Luc2 cells for 24 h. Surprisingly, NP12 (20% DETA)/siLuc2-C-LNP-CPP showed higher knockdown effect (~60 % knockdown) than other NP/siLuc2-C-LNP-CPP (~20% knockdown, **Figure 3b**). Although siRNA-C mixed with only CPP was also taken up into the cells (**Figure S5**), there was little knockdown effect. Since surface functionality (CPP modification) and particle size were not significantly different in each of the NP/siLuc2-C-LNP-CPP complexes, we assumed the siRNA uptake ratio should have been the same. However, the siRNA delivery ratio of NP12 (20% DETA)/siLuc2-C-LNP-CPP was lower than that of other NP/siLuc2-C-LNP-CPP complexes. We can only speculate at this point why this might be so. Perhaps some siRNA became detached from the NP12 (20% DETA) in the process of encapsulation of the NP12 (20% DETA) /siLuc2-C complex or some siRNA did not bind to NP12 (20% DETA). Furthermore, we confirmed that "naked" NP/siRNA-C complexes not encapsulated by LNPs were ineffective at delivering siRNA into cells (**Figure S7a,b**). As a result, the NP/siRNA complex (without LNP and CPP) showed no knockdown effect (**Figure S8**). These results establish that differences in the knockdown effect for each NP/siRNA-LNP-CPP complex arises from the differences in binding kinetics of siRNA to the NP and proton capacity of the NP. Although NP4 (20% APM) and NP8 (20% EDA) showed similar proton capacity to NP12 (20% DETA), siRNA showed relatively

low affinity for NP12 (20% DETA) at pH 7.4 (cytoplasm pH, K_d=128 nM) compared with NP4 (20% APM) (K_d=34 nM) and NP8 (20% EDA) (K_d=42 nM). Although 10% amine NPs (NP2,6,10) showed relatively low affinity at pH 7.4 (NP2 (10% APM): 114 nM, NP6 (10% EDA): 115 nM, NP10 (10% DETA): 186 nM) as well as NP12 (20% DETA), these NPs had low proton capacity compared with 20% amine NPs (NP4 (20% APM), 8 (20% EDA), 12 (20% DETA), **Figure S1**). Since NP12 (20% DETA) satisfied both factors, NP12 (20% DETA)/siLuc2-C-LNPCPP shows a higher knockdown effect than other NP/siLuc2-C-LNP-CPP complexes. Therefore, fast siRNA release kinetics from the NP at pH 7.4 and overall proton capacity of the NP are the important factors for efficient knockdown.

To demonstrate the effects of binding kinetics of the NPs to siRNA on intracellular distribution of siRNA, localization of siRNA and NPs in the cells was monitored by a confocal laser scanning microscope at 24 h after the addition (**Figure 3c**). TAMRA-conjugated siRNA-C was used and FITC labeled NPs were synthesized by the inclusion of FITC monomer into NPs (1 mol% in total monomer). Although most of the siRNA and NPs were co-localized in the cell by adding NP4 (20% APM) or 8 (20% EDA)/siLuc2-C-LNP-CPP (slow siRNA release), many siRNA and NPs were not co-localized by using NP12 (20% DETA)/siLuc2-C-LNP-CPP (fast siRNA release). These results indicate that NP12 (20% DETA) effectively and rapidly released siRNA into the cytoplasm compared with NP4 and NP8 (20% APM and EDA) resulting in significant knockdown. Since it was suggested that spacing and the number of amine residues is critical for NP−siRNA binding and induction of gene silencing,[38] we prepared EDA, APM and DETA monomers to evaluate these variables. Both EDA and APM containing NPs showed similar siRNA affinity and knockdown effect. However, DETA containing NPs behaved quite differently. These results indicate that spacing of amine residue in the mono-amine structure (APM and EDA) is not a critical factor for siRNA affinity and knockdown effect but the proximity of amines is critical. Increase of amine from one (APM and EDA) to two (DETA) significantly changes the siRNA affinity (k_{on} and k_{off}) and knockdown effect.

Since mono-amine functionalized NPs showed similar K_d between pH 5.5 (endosomal pH) and 7.4 (cytoplasm pH), siRNA cannot effectively detach from NPs in the cytoplasm. However, siRNA was effectively released from di-amine functionalized NPs into the cytoplasm, a result of the larger dissociation equilibrium constants at pH 7.4 compared to pH 5.5. This indicates that engineering k_{on}, k_{off} and K_d can be important for efficient knockdown in siRNA delivery by polycationic delivery systems. Until now, it was well known that the important factor of siRNA delivery vectors was the pK_a of the amine in the vector. We clearly showed that the importance is based on the change of dissociation equilibrium constants between pH 5.5 and 7.4.

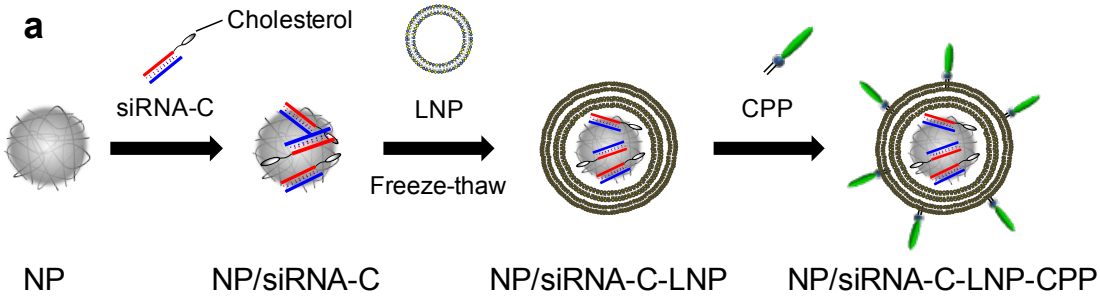
a
Cholesterol
siRNA-C
LNP
Freeze-thaw
CPP
NP
NP/siRNA-C
NP/siRNA-C-LNP
NP/siRNA-C-LNP-CPP

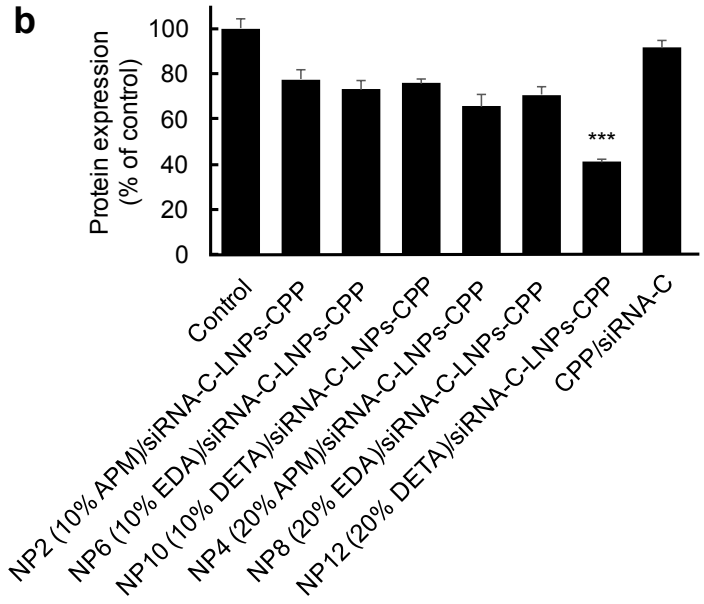
b
Protein expression
(% of control)
100
80
60
40
20
0
***
Control
NP2 (10% APM)/siRNA-C-LNPs-CPP
NP6 (10% EDA)/siRNA-C-LNPs-CPP
NP10 (10% DETA)/siRNA-C-LNPs-CPP
NP4 (20% APM)/siRNA-C-LNPs-CPP
NP8 (20% EDA)/siRNA-C-LNPs-CPP
NP12 (20% DETA)/siRNA-C-LNPs-CPP
CPP/siRNA-C

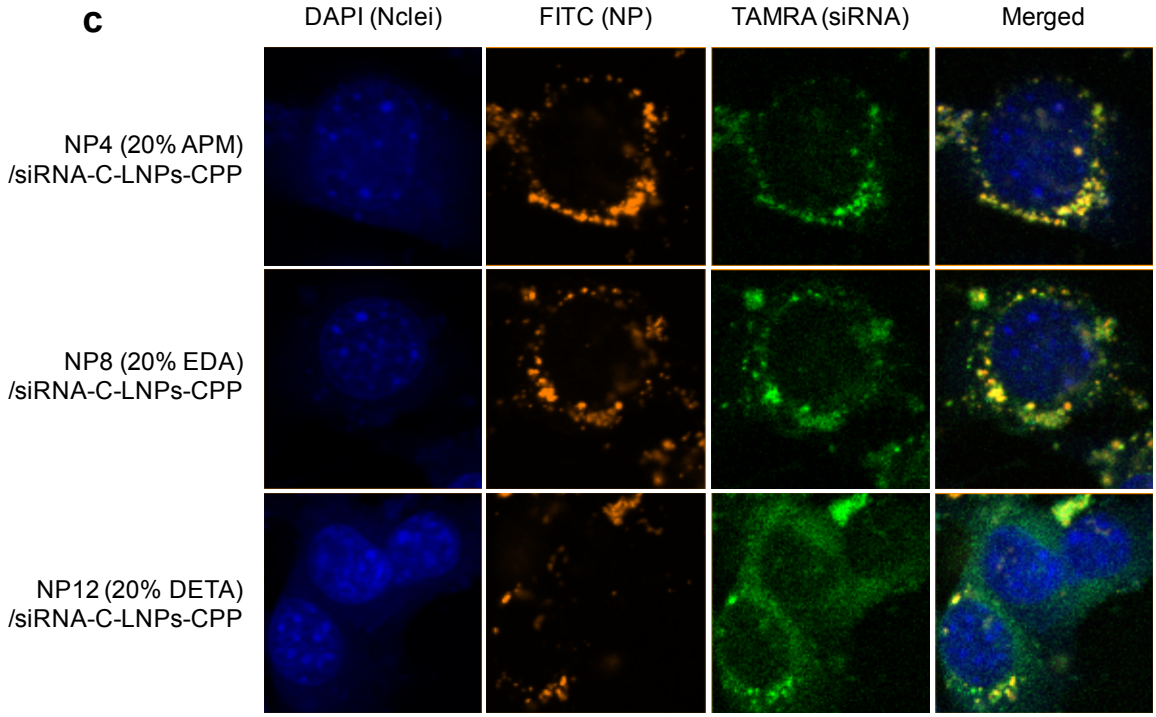
c
DAPI (Nclei)
FITC (NP)
TAMRA (siRNA)
Merged
NP4 (20% APM)
/siRNA-C-LNPs-CPP
NP8 (20% EDA)
/siRNA-C-LNPs-CPP
NP12 (20% DETA)
/siRNA-C-LNPs-CPP

Figure 3. Preparation of NP/siRNA-C-LNP-CPP and its knockdown effect. (a) Preparation of NP/siRNA-C-LNP-CPP. (b) Gene-silencing effect of NP/siRNA-C-LNP-CPP on B16F10-Luc2 cells. B16F10-Luc2 cells were incubated with NP/siRNA-C-LNP-CPP at a final siRNA concentration of 50 nM for 24 h. After the complexes were removed, the cells were cultured for an additional 24 h. Then, luciferase activities were measured and normalized by the total protein content. (***P<0.001, vs. NP2 (10% APM), 4 (20% APM), 6 (10% EDA), 8 (20% EDA), 10 (10 % DETA)/siRNA-LNP-CPP). (c) Confocal imaging of FITC-siRNA-C. Twelve hours after transfection of FITC-siRNA-C and NP4 (20% APM), NP8 (20% EDA) or NP12 (20% DETA)/siRNA-C-LNPs-CPP, the nuclei were stained with DAPI. The fluorescence intensity of FITC-siRNA-C taken up into the cells was observed. Colors are indicated as green for siRNA-C and blue for nuclei. Scale bars = 100 μm.

CONCLUSIONS

We conclude that siRNA association and dissociation rate constants (k_{on} and k_{off}) can be engineered by tuning the chemical composition and the structure of the synthetic polymer nanoparticle. An increase of the amine monomer percentage in the NP does not change the k_{on} but reduces the k_{off} of NPs. Dissociation equilibrium constants (K_d) of mono-amine functionalized NPs did not show a significant difference between pH 5.5 and 7.4. However, di-amine functionalized NPs showed larger K_d at pH 7.4 compared with pH 5.5. The relatively large dissociation equilibrium constants at pH 7.4 and small dissociation equilibrium constants at pH 5.5 results in a high knockdown effect. These results establish the importance of tuning the binding kinetics of NPs for target biomacromolecules for optimum efficacy. This is a first report to show direct evidence of the correlation between binding kinetics (k_{on} and k_{off}) of the siRNA delivery vector and knockdown effect.

ASSOCIATED CONTENT

Supporting Information.

The following files are available free of charge via the Internet at http://pubs.acs.org.

Evaluation of NP titration, interaction between cholesterol free siRNA and amine NPs, interaction between siRNA-C and several percentage of TBAm NPs, time courses of frequency changes of NP-immobilized QCM after addition of siRNA-C, size distributions of NPs and NP/siRNA-C-LNP-CPP, siRNA uptake using NP/siRNA-C-LNP-CPP and cytotoxicity of NPs or NP/siRNA-C-LNP-CPP.

Corresponding Author

Kenneth J. Shea, *Department of Chemistry, University of California Irvine, Irvine, CA 92697 USA,* E-mail: kjshea@uci.edu

Yu Hoshino, Department of Chemical Engineering, Kyushu University, 744 Motooka, Nishi-ku, Fukuoka, Fukuoka 819-0395 Japan, E-mail: yhoshino@chem-eng.kyushu-u.ac.jp

Author Contributions

The manuscript was written through contributions of all authors. All authors have given approval to the final version of the manuscript.

Funding Sources

This research was supported by JSPS and MEXT (20106003, 23111716 and 25107726) and in part by the National Science Foundation (DMR-1308363).

ACKNOWLEDGMENT

We thank Dr. T. Ozeki at Initium, Inc. for assistance with the QCM measurements. We also thank Dr, H. Matsune at Kyushu University for advice on the monomer synthesis.

ABBREVIATIONS

AIBN; 2,2'-azobis(isobutyronitrile), APM; (3-aminopropyl)methacrylamide hydrochloride, Bis; *N*,*N*'-methylenebis(acrylamide), CPP; cell penetrate peptide, CTAB; *N*,*N*,*N*',*N*'-tetramethylethylenediamine, hexadecyltrimethylammonium bromide, DCM; dichloromethane, DETA; diethylenetriamine, DOPE; dioleoylphosphatidylethanolamine, DPPG; 1,2-Dipalmitoyl-sn-glycero-3-phosphoglycerol, sodium salt, EDA; ethylenediamine, FBS; fetal bovine serum, LNP; lipid nanoparticle, NIPAm; *N*-isopropylacrylamide, NP; nanoparticle, QCM; quartz crystal microbalance, siRNA; small interfering RNA, TBAm; *N*-*tert*-butylacrylamide

REFERENCES

1. Nayak, S.; Lyon, L. A., Soft nanotechnology with soft nanoparticles. *Angew Chem Int Ed Engl* **2005,** 44, (47), 7686-708.
2. Cabaleiro-Lago, C.; Quinlan-Pluck, F.; Lynch, I.; Lindman, S.; Minogue, A. M.; Thulin, E.; Walsh, D. M.; Dawson, K. A.; Linse, S., Inhibition of amyloid beta protein fibrillation by polymeric nanoparticles. *J Am Chem Soc* **2008,** 130, (46), 15437-43.
3. Hoshino, Y.; Koide, H.; Urakami, T.; Kanazawa, H.; Kodama, T.; Oku, N.; Shea, K. J., Recognition, neutralization, and clearance of target peptides in the bloodstream of living mice by molecularly imprinted polymer nanoparticles: a plastic antibody. *J Am Chem Soc* **2010,** 132, (19), 6644-5.
4. Lee, S. H.; Hoshino, Y.; Randall, A.; Zeng, Z.; Baldi, P.; Doong, R. A.; Shea, K. J., Engineered synthetic polymer nanoparticles as IgG affinity ligands. *J Am Chem Soc* **2012,** 134, (38), 15765-72.
5. Yoshimatsu, K.; Lesel, B. K.; Yonamine, Y.; Beierle, J. M.; Hoshino, Y.; Shea, K. J., Temperature-responsive "catch and release" of proteins by using multifunctional polymer-based nanoparticles. *Angew Chem Int Ed Engl* **2012,** 51, (10), 2405-8.
6. Hoshino, Y.; Koide, H.; Furuya, K.; Haberaecker, W. W., 3rd; Lee, S. H.; Kodama, T.; Kanazawa, H.; Oku, N.; Shea, K. J., The rational design of a synthetic polymer nanoparticle that neutralizes a toxic peptide in vivo. *Proc Natl Acad Sci U S A* **2012,** 109, (1), 33-8.
7. Cedervall, T.; Lynch, I.; Foy, M.; Berggard, T.; Donnelly, S. C.; Cagney, G.; Linse, S.; Dawson, K. A., Detailed identification of plasma proteins adsorbed on copolymer nanoparticles. *Angew Chem Int Ed Engl* **2007,** 46, (30), 5754-6.
8. Cedervall, T.; Lynch, I.; Lindman, S.; Berggard, T.; Thulin, E.; Nilsson, H.; Dawson, K. A.; Linse, S., Understanding the nanoparticle-protein corona using methods to quantify exchange

rates and affinities of proteins for nanoparticles. *Proc Natl Acad Sci U S A* **2007,** 104, (7), 2050-5.
9. Sun, X.; Rossin, R.; Turner, J. L.; Becker, M. L.; Joralemon, M. J.; Welch, M. J.; Wooley, K. L., An assessment of the effects of shell cross-linked nanoparticle size, core composition, and surface PEGylation on in vivo biodistribution. *Biomacromolecules* **2005,** 6, (5), 2541-54.
10. Salvati, A.; Pitek, A. S.; Monopoli, M. P.; Prapainop, K.; Bombelli, F. B.; Hristov, D. R.; Kelly, P. M.; Aberg, C.; Mahon, E.; Dawson, K. A., Transferrin-functionalized nanoparticles lose their targeting capabilities when a biomolecule corona adsorbs on the surface. *Nat Nanotechnol* **2013,** 8, (2), 137-43.
11. Hoshino, Y.; Nakamoto, M.; Miura, Y., Control of protein-binding kinetics on synthetic polymer nanoparticles by tuning flexibility and inducing conformation changes of polymer chains. *J Am Chem Soc* **2012,** 134, (37), 15209-12.
12. Nakamoto, M.; Hoshino, Y.; Miura, Y., Effect of physical properties of nanogel particles on the kinetic constants of multipoint protein recognition process. *Biomacromolecules* **2014,** 15, (2), 541-7.
13. Hoshino, Y.; Urakami, T.; Kodama, T.; Koide, H.; Oku, N.; Okahata, Y.; Shea, K. J., Design of synthetic polymer nanoparticles that capture and neutralize a toxic peptide. *Small* **2009,** 5, (13), 1562-8.
14. Yonamine, Y.; Yoshimatsu, K.; Lee, S. H.; Hoshino, Y.; Okahata, Y.; Shea, K. J., Polymer nanoparticle-protein interface. Evaluation of the contribution of positively charged functional groups to protein affinity. *ACS Appl Mater Interfaces* **2013,** 5, (2), 374-9.
15. Weisman, A.; Chen, Y. A.; Hoshino, Y.; Zhang, H.; Shea, K., Engineering nanoparticle antitoxins utilizing aromatic interactions. *Biomacromolecules* **2014,** 15, (9), 3290-5.
16. Okishima, A.; Koide, H.; Hoshino, Y.; Egami, H.; Hamashima, Y.; Oku, N.; Asai, T., Design of Synthetic Polymer Nanoparticles Specifically Capturing Indole, a Small Toxic Molecule. *Biomacromolecules* **2019,** 20, (4), 1644-1654.
17. Lee, S. H.; Hoshino, Y.; Randall, A.; Zeng, Z. Y.; Baldi, P.; Doong, R. A.; Shea, K. J., Engineered Synthetic Polymer Nanoparticles as IgG Affinity Ligands. *Journal of the American Chemical Society* **2012,** 134, (38), 15765-15772.
18. Koide, H.; Tsuchida, H.; Nakamoto, M.; Okishima, A.; Ariizumi, S.; Kiyokawa, C.; Asai, T.; Hoshino, Y.; Oku, N., Rational designing of an antidote nanoparticle decorated with abiotic polymer ligands for capturing and neutralizing target toxins. *J Control Release* **2017,** 268, 335-342.
19. Koide, H.; Yoshimatsu, K.; Hoshino, Y.; Lee, S. H.; Okajima, A.; Ariizumi, S.; Narita, Y.; Yonamine, Y.; Weisman, A. C.; Nishimura, Y.; Oku, N.; Miura, Y.; Shea, K. J., A polymer nanoparticle with engineered affinity for a vascular endothelial growth factor (VEGF165). *Nat Chem* **2017,** 9, (7), 715-722.
20. Koide, H.; Yoshimatsu, K.; Hoshino, Y.; Ariizumi, S.; Okishima, A.; Ide, T.; Egami, H.; Hamashima, Y.; Nishimura, Y.; Kanazawa, H.; Miura, Y.; Asai, T.; Oku, N.; Shea, K. J., Sequestering and inhibiting a vascular endothelial growth factor in vivo by systemic administration of a synthetic polymer nanoparticle. *J Control Release* **2019,** 295, 13-20.
21. Wittrup, A.; Lieberman, J., Knocking down disease: a progress report on siRNA therapeutics. *Nat Rev Genet* **2015,** 16, (9), 543-52.
22. de Fougerolles, A.; Vornlocher, H. P.; Maraganore, J.; Lieberman, J., Interfering with disease: a progress report on siRNA-based therapeutics. *Nat Rev Drug Discov* **2007,** 6,, 443-453

23. Oku, N.; Yamazaki, Y.; Matsuura, M.; Sugiyama, M.; Hasegawa, M.; Nango, M., A novel non-viral gene transfer system, polycation liposomes. *Adv Drug Deliv Rev* **2001,** 52, (3), 209-18.
24. York, A. W.; Zhang, Y.; Holley, A. C.; Guo, Y.; Huang, F.; McCormick, C. L., Facile synthesis of multivalent folate-block copolymer conjugates via aqueous RAFT polymerization: targeted delivery of siRNA and subsequent gene suppression. *Biomacromolecules* **2009,** 10, (4), 936-43.
25. Nguyen, J.; Reul, R.; Roesler, S.; Dayyoub, E.; Schmehl, T.; Gessler, T.; Seeger, W.; Kissel, T. H., Amine-modified poly(vinyl alcohol)s as non-viral vectors for siRNA delivery: effects of the degree of amine substitution on physicochemical properties and knockdown efficiency. *Pharm Res* **2010,** 27, (12), 2670-82.
26. Uchida, H.; Miyata, K.; Oba, M.; Ishii, T.; Suma, T.; Itaka, K.; Nishiyama, N.; Kataoka, K., Odd-even effect of repeating aminoethylene units in the side chain of N-substituted polyaspartamides on gene transfection profiles. *J Am Chem Soc* **2011,** 133, (39), 15524-32.
27. Kim, S. I.; Shin, D.; Choi, T. H.; Lee, J. C.; Cheon, G. J.; Kim, K. Y.; Park, M.; Kim, M., Systemic and specific delivery of small interfering RNAs to the liver mediated by apolipoprotein A-I. *Mol Ther* **2007,** 15, (6), 1145-52.
28. Alabi, C. A.; Love, K. T.; Sahay, G.; Yin, H.; Luly, K. M.; Langer, R.; Anderson, D. G., Multiparametric approach for the evaluation of lipid nanoparticles for siRNA delivery. *Proc Natl Acad Sci U S A* **2013,** 110, (32), 12881-6.
29. Blackburn, W. H.; Dickerson, E. B.; Smith, M. H.; McDonald, J. F.; Lyon, L. A., Peptide-functionalized nanogels for targeted siRNA delivery. *Bioconjug Chem* **2009,** 20, (5), 960-8.
30. Nuhn, L.; Hirsch, M.; Krieg, B.; Koynov, K.; Fischer, K.; Schmidt, M.; Helm, M.; Zentel, R., Cationic nanohydrogel particles as potential siRNA carriers for cellular delivery. *ACS nano* **2012,** 6, (3), 2198-214.
31. Leber, N.; Nuhn, L.; Zentel, R., Cationic Nanohydrogel Particles for Therapeutic Oligonucleotide Delivery. *Macromolecular bioscience* **2017,** 17, (10).
32. Leber, N.; Kaps, L.; Aslam, M.; Schupp, J.; Brose, A.; Schaffel, D.; Fischer, K.; Diken, M.; Strand, D.; Koynov, K.; Tuettenberg, A.; Nuhn, L.; Zentel, R.; Schuppan, D., SiRNA-mediated in vivo gene knockdown by acid-degradable cationic nanohydrogel particles. *Journal of controlled release : official journal of the Controlled Release Society* **2017,** 248, 10-23.
33. Elsayed, M.; Corrand, V.; Kolhatkar, V.; Xie, Y. R.; Kim, N. H.; Kolhatkar, R.; Merkel, O. M., Influence of Oligospermines Architecture on Their Suitability for siRNA Delivery. *Biomacromolecules* **2014,** 15, (4), 1299-1310.
34. Yu, G. S.; Bae, Y. M.; Choi, H.; Kong, B.; Choi, I. S.; Choi, J. S., Synthesis of PAMAM Dendrimer Derivatives with Enhanced Buffering Capacity and Remarkable Gene Transfection Efficiency. *Bioconjugate Chem* **2011,** 22, (6), 1046-1055.
35. Lachelt, U.; Kos, P.; Mickler, F. M.; Herrmann, A.; Salcher, E. E.; Rodl, W.; Badgujar, N.; Brauchle, C.; Wagner, E., Fine-tuning of proton sponges by precise diaminoethanes and histidines in pDNA polyplexes. *Nanomed-Nanotechnol* **2014,** 10, (1), 35-44.
36. Jayaraman, M.; Ansell, S. M.; Mui, B. L.; Tam, Y. K.; Chen, J.; Du, X.; Butler, D.; Eltepu, L.; Matsuda, S.; Narayanannair, J. K.; Rajeev, K. G.; Hafez, I. M.; Akinc, A.; Maier, M. A.; Tracy, M. A.; Cullis, P. R.; Madden, T. D.; Manoharan, M.; Hope, M. J., Maximizing the potency of siRNA lipid nanoparticles for hepatic gene silencing in vivo. *Angew Chem Int Ed Engl* **2012,** 51, (34), 8529-33.
37. Okamoto, A.; Koide, H.; Morita, N.; Hirai, Y.; Kawato, Y.; Egami, H.; Hamashima, Y.; Asai, T.; Dewa, T.; Oku, N., Rigorous control of vesicle-forming lipid pKa by fluorine-

conjugated bioisosteres for gene-silencing with siRNA. *Journal of controlled release : official journal of the Controlled Release Society* **2019,** 295, 87-92.
38. Sun, W.; Bandmann, H.; Schrader, T., A fluorescent polymeric heparin sensor. *Chemistry* **2007,** 13, (27), 7701-7.
39. Yoshimatsu, K.; Koide, H.; Hoshino, Y.; Shea, K. J., Preparation of abiotic polymer nanoparticles for sequestration and neutralization of a target peptide toxin. *Nature protocols* **2015,** 10, (4), 595-604.
40. Koide, H.; Okamoto, A.; Tsuchida, H.; Ando, H.; Ariizumi, S.; Kiyokawa, C.; Hashimoto, M.; Asai, T.; Dewa, T.; Oku, N., One-step encapsulation of siRNA between lipid-layers of multi-layer polycation liposomes by lipoplex freeze-thawing. *J Control Release* **2016,** 228, 1-8.
41. Yue, M. C.; Hoshino, Y.; Miura, Y., Design rationale of thermally responsive microgel particle films that reversibly absorb large amounts of CO2: fine tuning the pK(a) of ammonium ions in the particles. *Chem Sci* **2015,** 6, (11), 6112-6123.
42. Wolfrum, C.; Shi, S.; Jayaprakash, K. N.; Jayaraman, M.; Wang, G.; Pandey, R. K.; Rajeev, K. G.; Nakayama, T.; Charrise, K.; Ndungo, E. M.; Zimmermann, T.; Koteliansky, V.; Manoharan, M.; Stoffel, M., Mechanisms and optimization of in vivo delivery of lipophilic siRNAs. *Nat Biotechnol* **2007,** 25, (10), 1149-57.
43. Whitehead, K. A.; Langer, R.; Anderson, D. G., Knocking down barriers: advances in siRNA delivery. *Nat Rev Drug Discov* **2009,** 8, (2), 129-38.
44. Hoshino, Y.; Ohashi, R. C.; Miura, Y., Rational design of synthetic nanoparticles with a large reversible shift of acid dissociation constants: proton imprinting in stimuli responsive nanogel particles. *Adv Mater* **2014,** 26, (22), 3718-23.
45. Benjaminsen, R. V.; Mattebjerg, M. A.; Henriksen, J. R.; Moghimi, S. M.; Andresen, T. L., The possible "proton sponge " effect of polyethylenimine (PEI) does not include change in lysosomal pH. *Molecular therapy : the journal of the American Society of Gene Therapy* **2013,** 21, (1), 149-57.
46. Suma, T.; Miyata, K.; Ishii, T.; Uchida, S.; Uchida, H.; Itaka, K.; Nishiyama, N.; Kataoka, K., Enhanced stability and gene silencing ability of siRNA-loaded polyion complexes formulated from polyaspartamide derivatives with a repetitive array of amino groups in the side chain. *Biomaterials* **2012,** 33, (9), 2770-9.
47. Freeman, E. C.; Weiland, L. M.; Meng, W. S., Modeling the proton sponge hypothesis: examining proton sponge effectiveness for enhancing intracellular gene delivery through multiscale modeling. *J Biomater Sci Polym Ed* **2013,** 24, (4), 398-416.
48. Hoshino, Y.; Haberaecker, W. W., 3rd; Kodama, T.; Zeng, Z.; Okahata, Y.; Shea, K. J., Affinity purification of multifunctional polymer nanoparticles. *J Am Chem Soc* **2010,** 132, (39), 13648-50.
49. Hu, C. M.; Fang, R. H.; Copp, J.; Luk, B. T.; Zhang, L., A biomimetic nanosponge that absorbs pore-forming toxins. *Nat Nanotechnol* **2013,** 8, (5), 336-40.
50. Hu, C. M.; Zhang, L.; Aryal, S.; Cheung, C.; Fang, R. H.; Zhang, L., Erythrocyte membrane-camouflaged polymeric nanoparticles as a biomimetic delivery platform. *Proceedings of the National Academy of Sciences of the United States of America* **2011,** 108, (27), 10980-5.
51. Litzinger, D. C.; Huang, L., Phosphatidylethanolamine liposomes: drug delivery, gene transfer and immunodiagnostic applications. *Biochim Biophys Acta* **1992,** 1113, (2), 201-27.
52. Heyes, J.; Palmer, L.; Bremner, K.; MacLachlan, I., Cationic lipid saturation influences intracellular delivery of encapsulated nucleic acids. *J Control Release* **2005,** 107, (2), 276-87.

53. Farhood, H.; Serbina, N.; Huang, L., The role of dioleoyl phosphatidylethanolamine in cationic liposome mediated gene transfer. *Biochim Biophys Acta* **1995,** 1235, (2), 289-95.
54. Dominska, M.; Dykxhoorn, D. M., Breaking down the barriers: siRNA delivery and endosome escape. *J Cell Sci* **2010,** 123, (Pt 8), 1183-9.
55. Asai, T.; Tsuzuku, T.; Takahashi, S.; Okamoto, A.; Dewa, T.; Nango, M.; Hyodo, K.; Ishihara, H.; Kikuchi, H.; Oku, N., Cell-penetrating peptide-conjugated lipid nanoparticles for siRNA delivery. *Biochem Biophys Res Commun* **2014,** 444, (4), 599-604.

Table of Contents graphic